Vitamin D ameliorates particulate matter induced mitochondrial damages and calcium dyshomeostasis in BEAS-2B human bronchial epithelial cells

Ju Chang-Chien[1,2], Jing-Long Huang[2,3,4], Hui-Ju Tsai[5,6], Shih-Ling Wang[1], Ming-Ling Kuo[1,3,7*] and Tsung-Chieh Yao[1,2,4*]

Abstract

Background Mitochondria is prone to oxidative damage by endogenous and exogenous sources of free radicals, including particulate matter (PM). Given the role of mitochondria in inflammatory disorders, such as asthma and chronic obstructive pulmonary disease, we hypothesized that supplementation of vitamin D may play a protective role in PM-induced mitochondrial oxidative damages of human bronchial epithelial BEAS-2B cells.

Methods BEAS-2B cells were pretreated with $1,25(OH)_2D_3$, an active form of vitamin D, for 1 h prior to 24-hour exposure to PM (SRM-1648a). Oxidative stress was measured by flow cytometry. Mitochondrial functions including mitochondrial membrane potential, ATP levels, and mitochondrial DNA copy number were analyzed. Additionally, mitochondrial ultrastructure was examined using transmission electron microscopy. Intracellular and mitochondrial calcium concentration changes were assessed using flow cytometry based on the expression of Fluo-4 AM and Rhod-2 AM, respectively. Pro-inflammatory cytokines, including IL-6 and MCP-1, were quantified using ELISA. The expression levels of antioxidants, including SOD1, SOD2, CAT, GSH, and NADPH, were determined.

Results Our findings first showed that 24-hour exposure to PM led to the overproduction of reactive oxygen species (ROS) derived from mitochondria. PM-induced mitochondrial oxidation resulted in intracellular calcium accumulation, particularly within mitochondria, and alterations in mitochondrial morphology and functions. These changes included loss of mitochondrial membrane integrity, disarrayed cristae, mitochondrial membrane depolarization, reduced ATP production, and increased mitochondrial DNA copy number. Consequently, PM-induced mitochondrial damage triggered the release of certain inflammatory cytokines, such as IL-6 and MCP-1. Similar to the actions of mitochondrial ROS inhibitor MitoTEMPO, $1,25(OH)_2D_3$ conferred protective effects on mtDNA alterations, mitochondrial damages, calcium dyshomeostasis, thereby decreasing the release of certain inflammatory cytokines. We found that greater cellular level of $1,25(OH)_2D_3$ upregulated the expression of enzymatic (SOD1, SOD2, and CAT) and non-enzymatic (GSH and NADPH) antioxidants to modulate cellular redox homeostasis.

*Correspondence:
Ming-Ling Kuo
mingling@mail.cgu.edu.tw
Tsung-Chieh Yao
yao@adm.cgmh.org.tw
Full list of author information is available at the end of the article

Conclusion Our study provides new evidence that 1,25(OH)$_2$D$_3$ acts as an antioxidant, enhancing BEAS-2B antioxidant responses to regulate mitochondrial ROS homeostasis and mitochondrial function, thereby enhancing epithelial defense against air pollution exposure.

Keywords Mitochondria, Mitochondrial DNA copy number, Oxidative stress, Particulate matter, Vitamin D

Background

Ambient air pollution poses a significant impact on human health. Exposure to the complex mixture of solid and liquid particles suspended in the air, such as particulate matter (PM), has been linked to several human health conditions, including declining lung function, asthma, chronic obstructive pulmonary disease (COPD), eczema, and cardiovascular disorders [15, 21, 22, 43]. One important mechanism is through induction of oxidative stress, which can disrupt multiple cellular processes, for example, inflammation, organelle dysfunction, cell death, and mitochondrial impairment [26, 29]. Given the widespread impact of PM exposure on human health, it is crucial to gain a better understanding of the underlying mechanisms.

Vitamin D plays a critical role in antioxidant, calcium homeostasis, and immune regulation [8, 23]. Previous studies have reported the association of vitamin D deficiency with detrimental lung function [42], chronic respiratory diseases [13], and atopic dermatitis [10], but the underlying mechanisms are not yet fully understood. To the best of our knowledge, the capacity of vitamin D affecting the lung response to PM toxicity remains unclear.

Mitochondria play a role in energy production and reactive oxygen species (ROS) regulation [1, 19, 36]. Previous studies have reported that mitochondria are particularly vulnerable to oxidative damage when ROS levels exceed endogenous antioxidant defense regulation [18, 20]. In response, the first-line defense antioxidant enzymes including superoxide dismutase (SOD), catalase (CAT) and glutathione peroxidase (GPX), as well as the reduced form of NADP$^+$ (or NADPH) become essential to maintain redox balance [18, 38]. Voltage-dependent anion channel 1 (VDAC-1), a component of the mitochondrial permeability transition pore (mTPT), has been demonstrated to be responsible for regulating the entry and exit of calcium and ROS into and out of mitochondria [11, 35]. Mitochondria serve as central hubs for intracellular calcium buffering, and the bidirectional interaction between calcium and ROS [14, 32].

Nowadays limited studies have examined the role of vitamin D in mitochondrial response to PM exposure in epithelial cells. We hypothesized that vitamin D supplementation provides protection against mitochondrial DNA (mtDNA) damage, mitochondrial malfunction and calcium dyshomeostasis through enhancement of antioxidant pathways in the context of PM exposure.

Methods

Preparation of PM, activated vitamin D and chemical reagents

SRM-1648a, ambient urban particulate matter, was purchased from the National Institute of Standards and Technology (NIST) in US and used in this study. These particles consist of fine and ultrafine particles with an aerodynamic diameter ranging from 1.35 to 30.1 μm (mean 5.85 μm) and are comprised of various polycyclic aromatic hydrocarbons (PAHs) and inorganic and organic elements such as iron, calcium and zinc. The stock suspension was prepared by 1-hour sonication in dimethyl sulfoxide (DMSO) to achieve a PM concentration of 100 mg/ml, following NIST's guidelines. The PM suspension was then stored at -80℃ before use. In addition, ROS scavengers including N-acetyl-L-cysteine (NAC; 1 μM) and MitoTEMPO (50 μM), as well as 1,25-dihydroxyvitamin D3 (1,25(OH)$_2$D$_3$), an active form of vitamin D, and antimycin A were obtained from Sigma-Aldrich and applied in subsequent in vitro exposure experiments.

Cell culture and treatment

Human BEAS-2B cell line, a non-tumorigenic bronchial epithelial cell line derived from human bronchial epithelium, was applied in this study. BEAS-2B cells were cultured in Dulbecco's Modified Eagle's Medium/ Nutrient Mixture F-12 (DMEM/F-12) supplemented with 10% heat-inactivated fetal bovine serum (FBS) and 1% penicillin/streptomycin antibiotics, and maintained in a humidified atmosphere of 95% air/ 5% CO$_2$ at 37℃. When cells reached about 80% confluence, they were exposed to different concentrations of PM suspended in serum-reduced media (DMEM/F-12 supplemented with 2% FBS) to evaluate their effects. The stock PM suspension underwent 1-hour sonication to break up most agglomerates before use. Furthermore, the in vitro exposure experiments were conducted and completed within 1 h of preparation to maintain consistency in PM size distribution. For experiments investigating the impact of vitamin D upon PM exposure, BEAS-2B cells were pretreated with 1,25(OH)$_2$D$_3$ in the serum-reduced media for 1 h prior to PM exposure. Control cells were cultured in medium containing 2% FBS and 0.1% DMSO.

Determination of intracellular and mitochondrial ROS production

Intracellular ROS levels in BEAS-2B cells were determined by fluorometric analysis using 2',7'-dichlorodihydrofluorescein diacetate (DCF-DA; Roche), while mitochondrial ROS levels were examined using MitoSOX red mitochondrial superoxide indicator (Thermo Fisher Scientific). After treatment with PM and/or $1,25(OH)_2D_3$, the culture media were removed, and the cells were stained with 10 µM DCF-DA in serum-free media or 5 µM MitoSOX red dye in Hanks' Balanced Salt Solution (HBSS) containing Ca^{2+} and Mg^{2+} for 20 min at 37℃ in the dark. Following staining, the cells were harvested in cold phosphate-buffered saline (PBS) solution and fluorescence intensity was analyzed using a FACSCanto II flow cytometry (BD Biosciences). Fluorescent signals were recorded for 10,000 cells. Intracellular ROS results were expressed as fold change in mean fluorescence intensity (MFI) relative to controls, while the percentage of MitoSOX red positive cells was used to quantify mitochondrial ROS.

Water-soluble tetrazolium-1 assay

Water-soluble tetrazolium 1 (WST-1) assay is widely utilized for evaluating the metabolic activity of viable cells and cell proliferation, following the guidelines provided by the manufacturer (Roche).

Assessment of mitochondrial membrane potential

We used JC-1, a lipophilic, cationic, dual-emission fluorescent dye from Thermo Fisher Scientific, to detect BEAS-2B cells with impaired mitochondrial membrane potential (mtMP). In healthy cells with polarized mitochondria (normal mtMP), JC-1 forms red fluorescent J-aggregates. In contrast, in damaged cells with depolarized mitochondria (low mtMP), JC-1 remains in its monomeric form, emitting green fluorescence. Briefly, BEAS-2B cells were seeded in 6-well plates and subjected to the following treatments for 24 h: PM alone, PM combined with $1,25(OH)_2D_3$, antimycin A alone or Antimycin A combined with $1,25(OH)_2D_3$. After the treatments, cells were then stained with JC-1 dye (2 µM JC-1 in 1x PBS) and incubated for 20 min at 37℃ in the dark. The fluorescence intensity of JC-1 aggregates and monomers was detected by flow cytometry (FACSCanto II; BD Biosciences) at excitation/emission wavelengths of 514/590 nm and 514/529 nm, respectively. The ratio of red to green fluorescence was used to determine mtMP, expressed as a percentage relative to the controls.

Intracellular ATP level detection

We used a colorimetric assay kit (Abcam ab83355) to measure cellular ATP levels. Following PM and/or $1,25(OH)_2D_3$ treatment, we harvested 1×10^6 cells, rinsed them in cold PBS, and homogenized them in ATP Assay Buffer. After centrifugation at 13,000 g for 5 min at 4℃, we mixed 50 µl of the supernatant with 50 µl of ATP reaction mix. Once the reaction was complete, we measured the absorbance at OD570 nm using a Synergy HTX microplate reader (BioTek). The ATP content of the cell lysate supernatant was determined using an ATP standard curve.

Transmission electron microscopy

The mitochondrial morphology in BEAS-2B cells were analyzed using transmission electron microscopy. Briefly, BEAS-2B cells were harvested after exposure to PM with or without $1,25(OH)_2D_3$ pretreatment for 24 h and rinsed three times with PBS. The cells were immediately fixed with a solution containing 3% glutaraldehyde and 2% paraformaldehyde in 0.1 M cacodylate buffer (pH 7.4) for 2 h at 4℃, followed by post-fixation in 1% osmium tetroxide solution for 1 h at 4℃. Subsequently, the cells were dehydrated using a graded ethanol series and embedded in 100% Epon resin. Thin sections of the embedded cells (approximately 80 nm thick) were prepared and stained with 4% uranyl acetate in H_2O for 2 h, followed by lead citrate for 10 min. Finally, the stained samples were examined using a HITACHI HT-7800 transmission electron microscopy.

Intracellular calcium flux measurement

Changes in intracellular calcium concentration were measured using Fluo-4 acetoxymethyl ester (Fluo-4 AM; Thermo Fisher Scientific), a cell-permeable, green-fluorescent calcium indicator. Fluo-4 AM is cleaved by cellular esterases in live cells to release free Fluo-4, which increases in fluorescence upon binding to calcium ions, with an excitation/emission wavelength of 494/506 nm. BEAS-2B cells (1×10^6 cells/ml) were stained with 1 µM Fluo-4 AM in PBS buffer for 30 min at 37℃, and then washed with PBS buffer to remove excess unincorporated dye. The time course of Fluo-4 fluorescence in BEAS-2B cells was recorded as the ratio of the fluorescent levels without stimulation for 90 s (baseline signal) and during exposure to PM for 360 s using flow cytometry (FACSCanto II; BD Biosciences). The area under the curve (AUC) of the calcium flux signal was calculated for exposure to PM for 360 s after background subtraction using the FlowJo v7.6 software. Intracellular calcium levels were expressed as the corresponding AUC values.

Mitochondrial calcium measurement

The positive charge of the fluorophore rhodamine-2-acetoxymethyl ester (Rhod-2 AM; Thermo Fisher Scientific) facilitates its sequestration into mitochondria, allowing it to monitor mitochondrial calcium concentration in BEAS-2B cells [6]. For flow cytometry analysis, cells were

harvested and suspended in PBS containing 1 μM Rhod-2 AM, followed by incubation of the cells in the dark for 30 min at 37℃. Mitochondrial calcium levels were then assessed using the FACSCanto II flow cytometer system from BD Biosciences, with an excitation/emission wavelength of 552/581 nm.

Cellular redox homeostasis
After PM and/or $1,25(OH)_2D_3$ treatment, cell were subjected to two freeze-thaw cycles (15 min on -80℃ followed by 10 min at room temperature) in the extraction buffer, and then centrifuged at 13,000 g for 20 min to remove cell debris. The supernatant was collected to quantify $NADP^+$/NADPH and GSH/GSSG ratios using commercial assay kits. Total amounts of NADPt ($NADP^+$ and NADPH) and NADPH were measured at OD450 nm, and the fluorescence intensity of total glutathione (GSH and GSSG) and GSH alone was monitored at an excitation/emission (Ex/Em) wavelength of 490/520 nm using a Synergy HTX microplate reader (BioTek). All procedures were conducted in accordance with the manufacturer's instructions, using kits such as the GSH/GSSG Ratio Detection Assay Kit II (Abcam ab205811) for GSH/GSSG quantification and the NADP/NADPH Assay Kit (Abcam ab65349) for $NADP^+$/NADPH assays.

Cytokine measurement
BEAS-2B cells were subjected to the following treatments for 24 h: PM alone, PM combined with $1,25(OH)_2D_3$, antimycin A alone or Antimycin A combined with $1,25(OH)_2D_3$. After the treatments, culture supernatants were stored at -80℃ pending measurement of secreted cytokine (IL-6) and chemokine (MCP-1), respectively. Concentrations of IL-6 and MCP-1 were detected in the conditioned culture supernatant by ELISA according to the manufacturer's instructions (R&D).

Assessment of mitochondrial DNA copy number
A PCR based method was conducted to assess mitochondrial DNA copy number (mtDNA-CN) as previously described [30]. Total DNA was extracted using a DNA extraction kit (RBC Bioscience), and mtDNA-CN was measured by real time qPCR assay (Bio-Rad CFX96) when the A260/A280 ratio of DNA reached 1.8-2.0. Primer sequences for *B2M* (for nuclear DNA) and $tRNA^{Leu(UUR)}$ (for mitochondrial DNA) genes are shown in Table S1. The cycle threshold (Ct) values for the two genes were obtained from triplicate reactions, and the difference in Ct values (ΔCt) between *B2M* and $tRNA^{Leu(UUR)}$ was calculated to determine the relative mtDNA-CN using the following formula: $2 \times 2^{\Delta Ct}$.

Antioxidant gene expression analysis
The $2^{-\Delta\Delta Ct}$ method was utilized to calculate the relative changes in antioxidant gene expression of *CAT*, *SOD1* and *SOD2*, with and without treatment of $1,25(OH)_2D_3$. Total RNA was isolated using TRIzol reagent (Sigma-Aldrich), followed by cDNA synthesis using 2.5 μg of total RNA reverse transcribed with a commercial RNA to cDNA EcoDry Premix kit (TakaRa). SYBR green-based real time qPCR was performed using a Bio-Rad CFX96 Real-Time PCR system. Primers for target and reference genes are provided in Table S1.

Statistical analysis
We performed statistical tests using the GraphPad Prsim 5.0 software program. All data were presented as mean±standard deviation (SD) of three independent experiments. Statistical differences among multiple groups were tested by one-way analysis of variance (ANOVA), followed by posterior comparisons using Dunnett's test. P-values less than 0.05 were considered statistically significant.

Results
PM exposure led to concentration- and time-dependent overproduction of ROS in BEAS-2B cells
We utilized the oxidation-sensitive DCF-DA dye to measure fluorescence intensity and assess whether PM induced intracellular ROS in BEAS-2B cells. We observed a concentration- and time-dependent effect of PM exposure on intracellular ROS generation in BEAS-2B cells. Figure 1A shows a 1.91±0.19-fold increase in ROS levels after a 24-hour exposure to 100 μg/ml of PM ($P<0.001$). We also observed a significant increase in ROS levels after just 1 h of exposure to 100 μg/ml of PM, with further increases observed from 1 to 24 h (Fig. 1B). Treatment with NAC, a well-known ROS scavenger and glutathione (GSH) precursor, significantly decreased intracellular ROS levels induced by 24-hour PM exposure (Fig. 1C). The WST-1 assay demonstrated a reduction in viable cell count following exposure to PM, accompanied by a decline in mitochondrial dehydrogenase activity (Fig. 1D). These findings suggest that PM exposure reduces cell metabolic activity and significantly increases the production of intracellular ROS in BEAS-2B cells. The corresponding PM concentrations, 50 μg/ml and 100 μg/ml, were used to further investigate the correlation between PM-induced oxidative stress and mitochondrial damages, as well as to evaluate the protective effects of vitamin D.
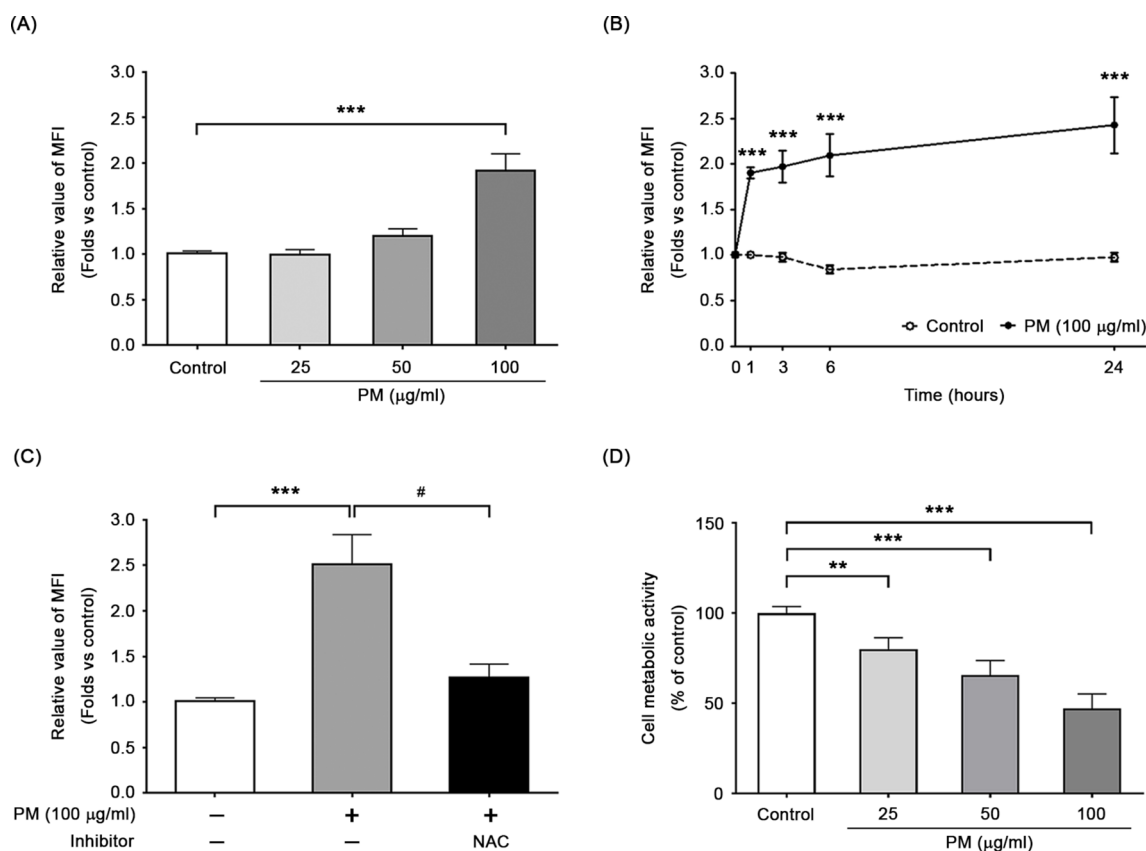
Chang-Chien *et al. Respiratory Research*   (2024) 25:321

Page 5 of 14

Fig. 1 PM induced intracellular ROS formation in BEAS-2B cells. Intracellular ROS formation was detected using DCF-DA dye. The concentration (**A**) and time (**B**) dependent increases in the levels of intracellular ROS were observed. (**C**) ROS scavenger, NAC, significantly inhibited PM-induced ROS production in BEAS-2B cells. (**D**) In addition, the WST-1 assay was employed to assess metabolic activity of cells following exposure to PM. $^{***}P < 0.001$ and $^{**}P < 0.01$, compared with untreated cells (control); $^{\#\#}P < 0.01$ and $^{\#}P < 0.05$, compared with the PM-stimulated group ($n = 3$)

PM-induced mitochondrial oxidative stress impaired mitochondrial function and increased mitochondrial DNA copy number

To investigate the effect of PM exposure on mitochondrial oxidative stress, we employed MitoSOX-derived red fluorescence to label BEAS-2B cells. Figure 2A demonstrates that PM exposure markedly increased mitochondrial ROS generation in a dose-dependent manner. The percentage of MitoSOX-positive cells treated with a PM concentration of 50 µg/ml or 100 µg/ml was significantly higher compared to control BEAS-2B cells ($P < 0.001$). Treatment with either NAC or MitoTEMPO, an inhibitor of mitochondrial ROS, resulted in a reduction of mitochondrial ROS formation in PM-exposed cells (Fig. 2B). Moreover, supplementation with MitoTEMPO led to a decrease in intracellular ROS levels and restored back to baseline levels (Fig. 2C).

To further investigate the relationship between PM-induced mitochondrial ROS overproduction and mitochondrial function in BEAS-2B cells, we evaluated the mtMP levels, intracellular ATP, and mtDNA-CN in the presence or absence of MitoTEMPO. Figure 2D demonstrates that 24-hour exposure to PM caused mtMP

dissipation, as evidenced by an increase in green fluorescence and a concomitant disappearance of red fluorescence. A decrement in the ratio of red/green fluorescence intensity, 58.62±13.15, 49.87±11.46, and 34.42±4.14, was observed in BEAS-2B cells exposed to increasing PM concentrations of 25, 50 and 100 µg/ml, respectively (Fig. 2E). We observed a significant decreasing trend of intracellular ATP levels in BEAS-2B cells when exposed to increasing PM concentration (Fig. 2F). Additionally, changes in mtDNA-CN following PM exposure were determined by qPCR. We observed a dose-dependent increase in mtDNA-CN while exposed BEAS-2B cells to PM for 24 h, with a 1.71±0.23-fold increase at 100 µg/ml ($P < 0.01$) compared to the controls (Fig. 2G). Treatment with MitoTEMPO significantly restored mtMP and mtDNA-CN levels and partially increased ATP production in cells exposed to PM (Fig. 2D to G). These results provide supportive evidence about the involvement of mitochondria in PM-induced cell damage, highlighting the critical impact of mitochondrial oxidative stress on mitochondrial function.
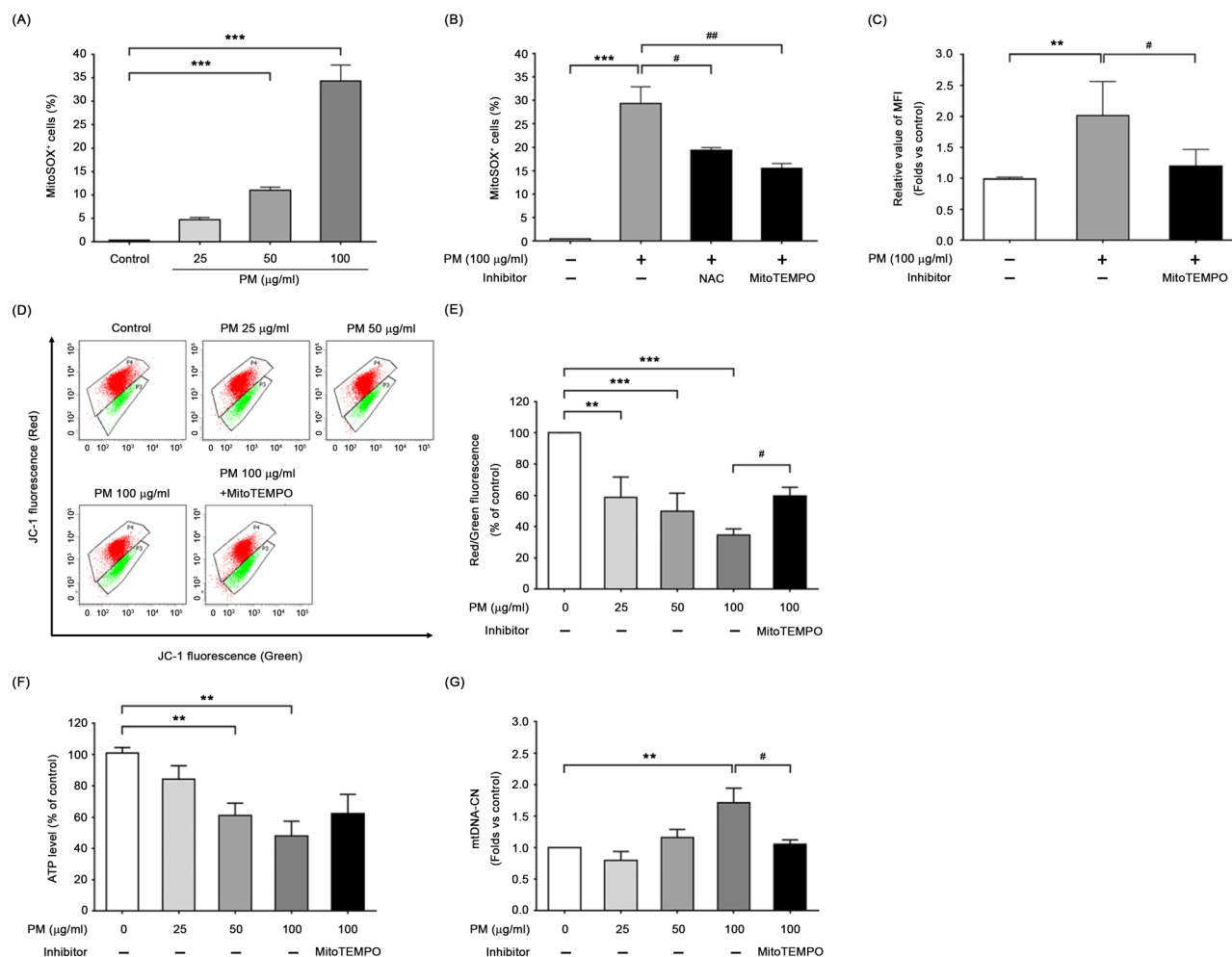
Fig. 2 Exposure to PM caused mitochondrial oxidative stress and mitochondrial dysfunction in BEAS-2B cells. (**A**) Mitochondrial ROS production was increased dose-dependently. PM exposure increased the MitoSOX-detected red fluorescence intensity in BEAS-2B cells, but (**B**) pretreatment with NAC or MitoTEMPO (as mitochondria-targeted antioxidant) could significantly reduce the level of mitochondrial ROS. (**C**) Moreover, MitoTEMPO pretreatment also led to a decrease in intracellular ROS levels. Changes in (**D**, **E**) mitochondrial membrane potential (mtMP) determined as a red/green fluorescence ratio with JC-1 staining, (**F**) intracellular ATP levels and (**G**) mitochondrial DNA copy number (mtDNA-CN) were observed after PM exposure in the absence or presence of MitoTEMPO. Data are means ± SD of three independent experiments, and significant differences were expressed as followed: $^{***}P < 0.001$ and $^{**}P < 0.01$, compared with untreated cells (control); $^{##}P < 0.01$ and $^{#}P < 0.05$, compared with the PM-stimulated group

1,25(OH)₂D₃ improved PM-induced mitochondrial dysfunction through antioxidant capacity

The antioxidant properties of 1,25(OH)$_2$D$_3$ were assessed by administering 10^{-1}-10 nM of the compound to BEAS-2B cells before PM exposure, and the results were shown in Fig. 3A and B. Both mitochondrial and intracellular ROS generations were significantly decreased, indicating that 1,25(OH)$_2$D$_3$ effectively counteracted PM-induced ROS overproduction in BEAS-2B cells. When exposed to PM for 24 h, pretreatment with 1,25(OH)$_2$D$_3$ at a concentration of 10 nM resulted in increased mtMP (Fig. 3C) and ATP content (Fig. 3D) compared to cells exposed to PM alone. The mtDNA-CN in BEAS-2B cells supplemented with 1,25(OH)$_2$D$_3$ was substantially restored compared to the control levels (Fig. 3E). Additionally, pretreatment with 1,25(OH)$_2$D$_3$ restored the count of

viable cells (Fig. 3F), and reduced the number of early apoptotic cells, as indicated by the Q4 quadrant, in PM-exposed BEAS-2B cells (Figure S1). These findings suggest that 1,25(OH)$_2$D$_3$ protects mitochondria away from PM-induced oxidative damages through its antioxidant property.

1,25(OH)₂D₃ restored PM-induced mitochondrial morphological changes

The structural morphology of mitochondria in BEAS-2B cells exposed to PM, both with and without 1,25(OH)$_2$D$_3$ treatment, were evaluated using transmission electron microscope (TEM). As illustrated in Fig. 4A and D, control BEAS-2B cells displayed heterogeneous mitochondrial shape (rounded or elongated) with intact mitochondrial membranes consisting of inner and outer
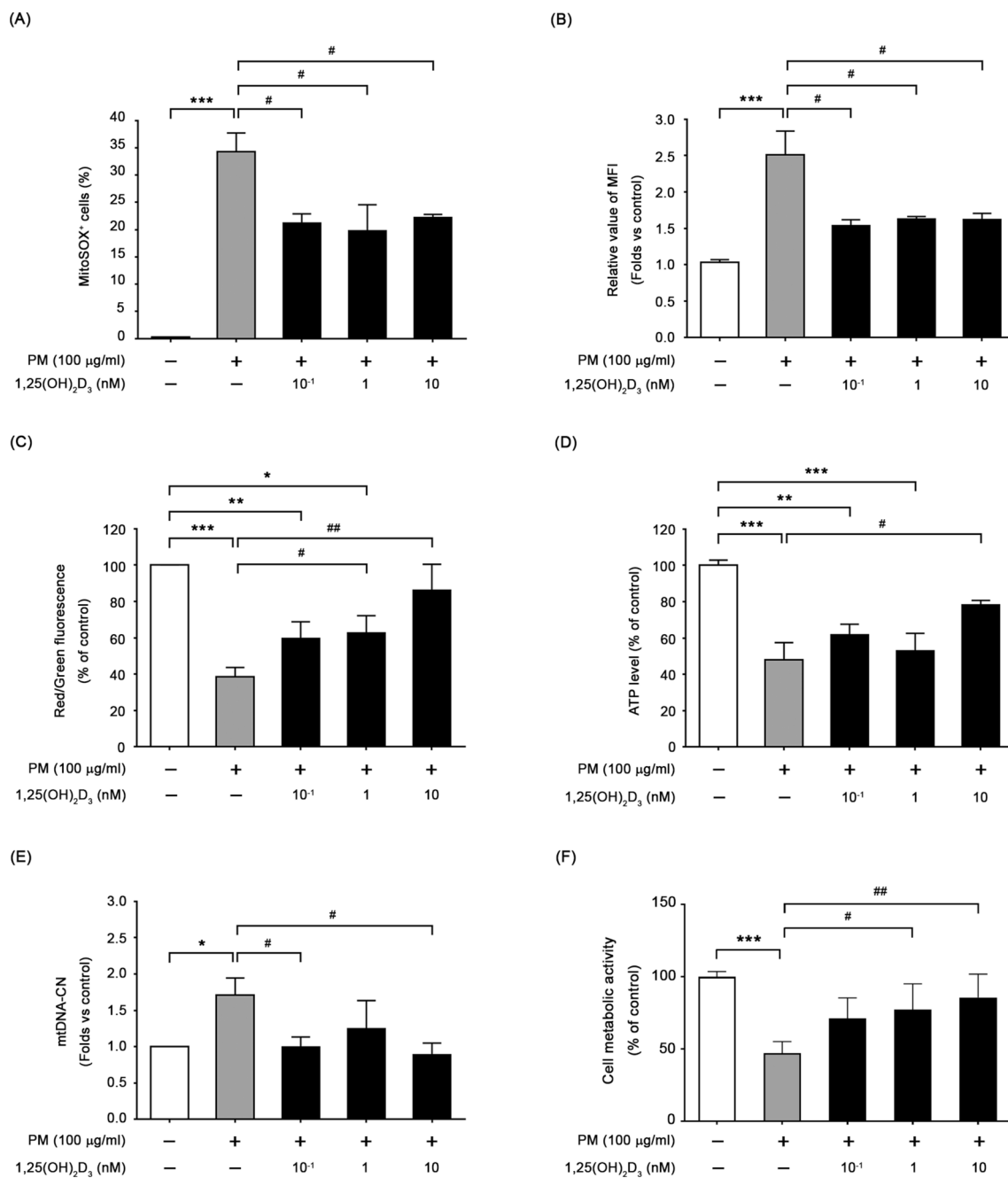
Fig. 3 1,25(OH)$_2$D$_3$ protected BEAS-2B from oxidative stress, leading to improve mitochondrial function in cells. Pretreatment with 1,25(OH)$_2$D$_3$ for 1 h before PM exposure, the levels of mitochondrial ROS (**A**), intracellular ROS (**B**), mtMP (**C**), ATP (**D**), mtDNA-CN (**E**) and cell viability (**F**) were measured in BEAS-2B cells, respectively. ***$P < 0.001$ and **$P < 0.01$ vs. untreated cells (control); ##$P < 0.01$ and #$P < 0.05$ vs. PM-stimulated group ($n = 3$)

membranes and extensively folded cristae. However, PM exposure led to changes in mitochondrial morphology, including altered membrane structural integrity with disorganized cristae and reduced electron density of the matrix (Fig. 4B and E). In contrast, pretreatment with 1,25(OH)$_2$D$_3$ restored mitochondrial matrix integrity in PM-exposed cells, although some mitochondria still showed disarrayed cristae (Fig. 4C and F). Overall, these

findings support 1,25(OH)$_2$D$_3$ mitigates the deleterious effects of PM on mitochondrial structure.

1,25(OH)$_2$D$_3$ eliminated PM-induced calcium dyshomeostasis

We investigated the impact of PM on intracellular calcium homeostasis via measuring intracellular calcium concentration using the calcium-sensitive dye, Fluo-4 AM, which produces changes in fluorescence intensity
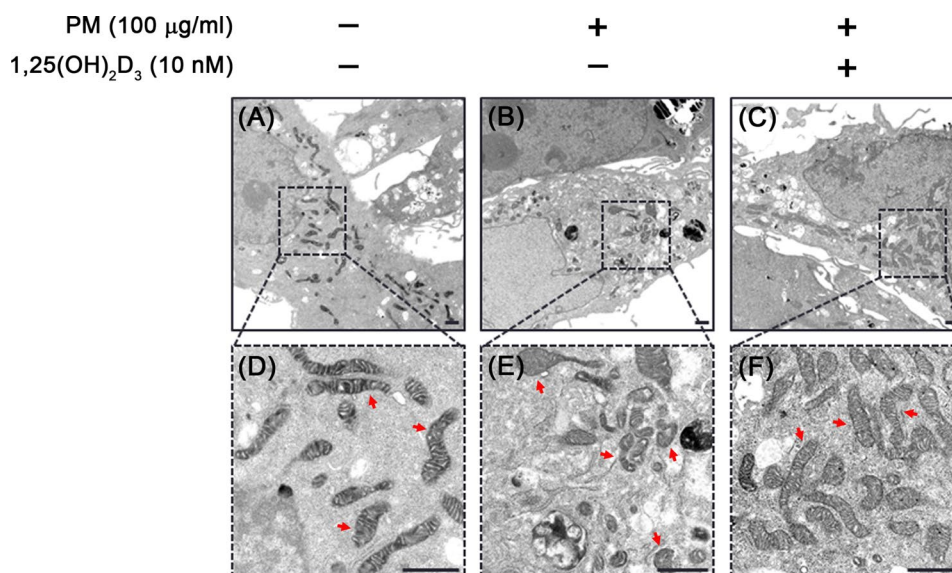
| PM (100 µg/ml) | − | + | + |
| 1,25(OH)$_2$D$_3$ (10 nM) | − | − | + |

Fig. 4 1,25(OH)$_2$D$_3$ restored PM-mediated alterations of mitochondrial ultrastructure in BEAS-2B cells. Cells treated with PM and 1,25(OH)$_2$D$_3$ for 24 h were subjected to transmission electron microscopy (TEM) analysis and mitochondrial morphology was compared (red arrow). (**A**, **D**) Control cells showed the integrity of mitochondrial membrane and the mitochondrial cristae. (**B**, **E**) Cells exposed to PM induced impaired mitochondrial membrane integrity and disarrayed cristae were observed. (**C**, **F**) The presence of 1,25(OH)$_2$D$_3$ could oppose the impact of PM on the mitochondrial morphology and restored it. Scale bar, 1 µm

corresponding to changes in intracellular calcium levels. We calculated AUC of the calcium levels for the first 360 s of PM stimulation after background subtraction. As shown in Fig. 5A and B, exposure to different concentrations of PM resulted in a transient rise in intracellular calcium levels, while no calcium flux was observed in the control cells. On the other hand, the inhibition of PM-induced calcium flux by ROS scavengers, such as Mito-TEMPO or NAC, was shown a significant reduction in the AUC (Fig. 5C). Similarly, treatment with 1,25(OH)$_2$D$_3$ led to a significant decrease in the excessive accumulation of intracellular calcium induced by PM, with observed intracellular calcium levels resembling those in the control cells (Fig. 5D). After 24 h of exposure to PM, live cells staining with Rhod-2 AM revealed significantly elevated mitochondrial calcium levels in PM-exposed BEAS-2B cells compared to the control cells, which were restored by treating with 1,25(OH)$_2$D$_3$ (Fig. 5E and F). Additionally, 1,25(OH)$_2$D$_3$ appeared to restore certain degree of the increase of VDAC-1 protein expression in mitochondrial fractions of PM-exposed cells (Figure S2). These findings clearly demonstrate that PM-induced excess ROS leads to elevated intracellular calcium levels, particularly within mitochondria; moreover, 1,25(OH)$_2$D$_3$ restores PM-induced calcium dyshomeostasis in BEAS-2B cells.

1,25(OH)$_2$D$_3$ reversed PM-induced cellular redox imbalance
In Fig. 6A to C, we observed a significant increase in the expression of three oxidative stress-related genes, *CAT*, *SOD1* and *SOD2*, in response to 1,25(OH)$_2$D$_3$ treatment. To further investigate the effects of 1,25(OH)$_2$D$_3$ on cellular redox environment in PM-exposed cells, we evaluated the levels of reduced glutathione (GSH) and the ratio of oxidized to reduced forms of NADPt (NADP$^+$/NADPH). Figure 6D and E showed that PM led to a significant decrease in GSH levels and an increase in the NADP$^+$/NADPH ratio when compared to control cells, and 1,25(OH)$_2$D$_3$ treatment restored both GSH levels and the NADP$^+$/NADPH ratio. These findings suggest that 1,25(OH)$_2$D$_3$ upregulates antioxidant gene expression and reverses redox imbalance in cells through its modulation of ROS overproduction induced by PM exposure.

Protective effects of 1,25(OH)$_2$D$_3$ on PM-induced inflammatory response
The impact of PM on the expression levels of pro-inflammatory cytokine (IL-6) and chemokine (MCP-1) in BEAS-2B cells was investigated. As shown in Fig. 7, a dose-dependent increase in inflammatory response was observed following PM exposure. PM exposure (100 µg/ml, 24 h) triggered an increase in production of IL-6 (1.76±0.11-fold; Fig. 7A) and MCP-1 (1.35±0.05-fold; Fig. 7B), separately, compared to the controls. Treatment with 1,25(OH)$_2$D$_3$ (1 and 10 nM) significantly suppressed the production of both IL-6 (Fig. 7C) and MCP-1 (Fig. 7D) in PM-exposed cells. On the other hand, addition of 1,25(OH)$_2$D$_3$ restored the levels of inflammatory cytokines and mitigated the decrease in mitochondrial membrane potential induced by antimycin A, which
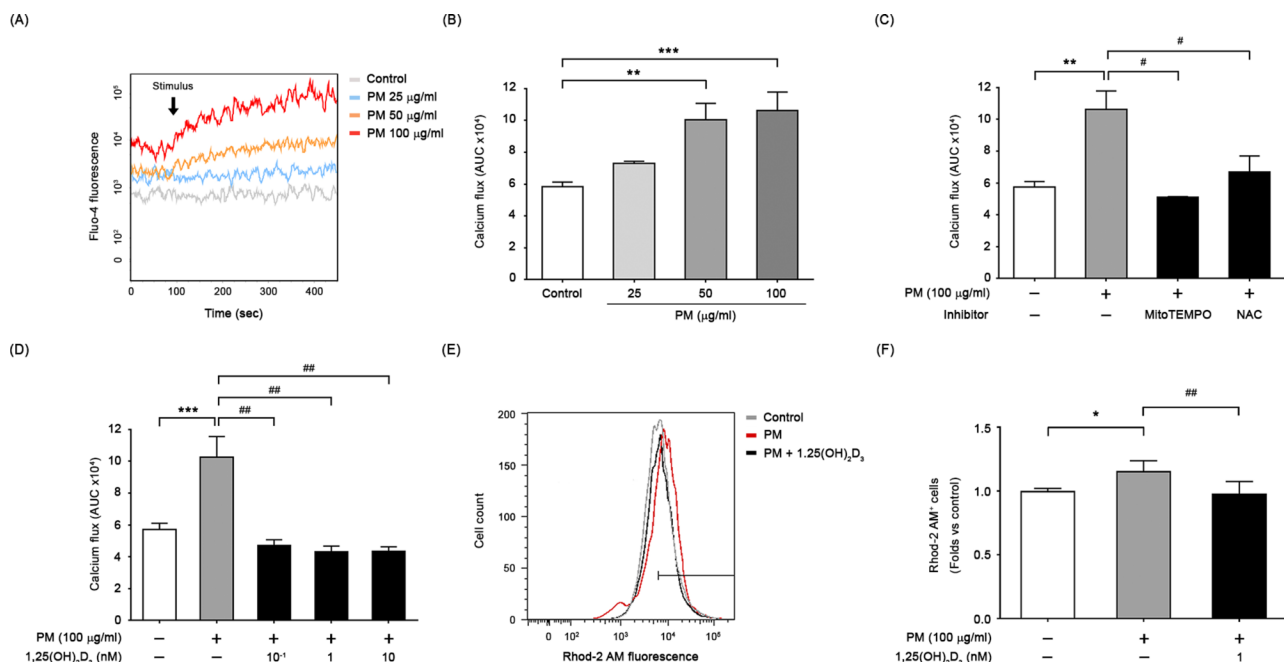
Fig. 5 1,25(OH)$_2$D$_3$ ameliorated the accumulation of intracellular and mitochondrial calcium caused by PM in BEAS-2B cells. (**A**) Changes in Fluo-4 fluorescence, representing changes in intracellular calcium levels, were measured at baseline (for 90 s) and after PM stimulation (indicated by the arrow; for 360 s). Representative graphs are shown. (**B**) The area under curve (AUC) of the calcium flux was calculated for the 360 s of PM stimulation after background subtraction, and presented as mean ± SD of three independent experiments. The beneficial effects of (**C**) antioxidants or (**D**) 1,25(OH)$_2$D$_3$ on calcium deregulation in cells exposed to PM were shown. (**E, F**) 1,25(OH)$_2$D$_3$ restored PM-induced elevation in mitochondrial calcium level, measured by flow cytometry using Rhod-2 AM. $^{***}P < 0.001$ and $^{**}P < 0.01$ vs. untreated cells (control); $^{##}P < 0.01$ and $^{#}P < 0.05$ vs. PM-stimulated group (n = 3)
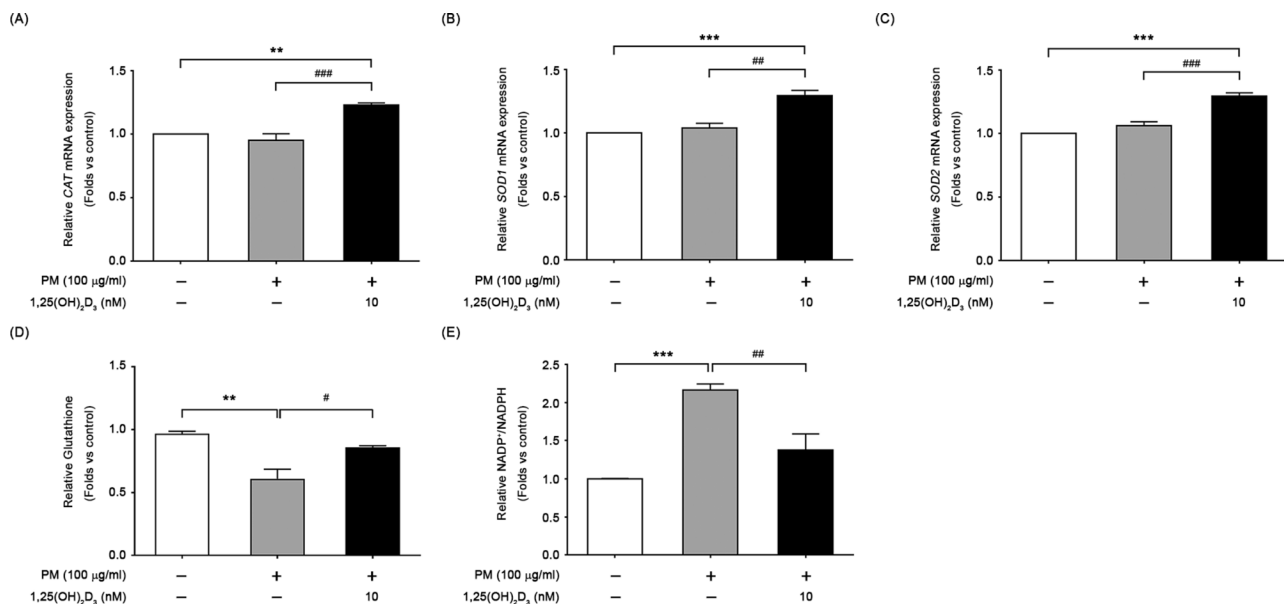

Fig. 6 Effects of 1,25(OH)$_2$D$_3$ on antioxidant capacity and cellular redox homeostasis. Expression of three oxidative stress related genes, (**A**) *CAT*, (**B**) *SOD1*, and (**C**) *SOD2*, in 6-hour cultures of BEAS-2B exposed to 100 µg/ml PM with or without 1,25(OH)$_2$D$_3$. In addition, after 24 h, the levels of (**D**) GSH, and (**E**) the ratio of oxidized to reduced NADP (NADP$^+$/NADPH) in cells were measured. Data were mean ± SD of three independent experiments. $^{***}P < 0.001$ and $^{**}P < 0.01$ in comparison with untreated cells (control); $^{###}P < 0.05$ and $^{##}P < 0.05$ in comparison with PM-stimulated group
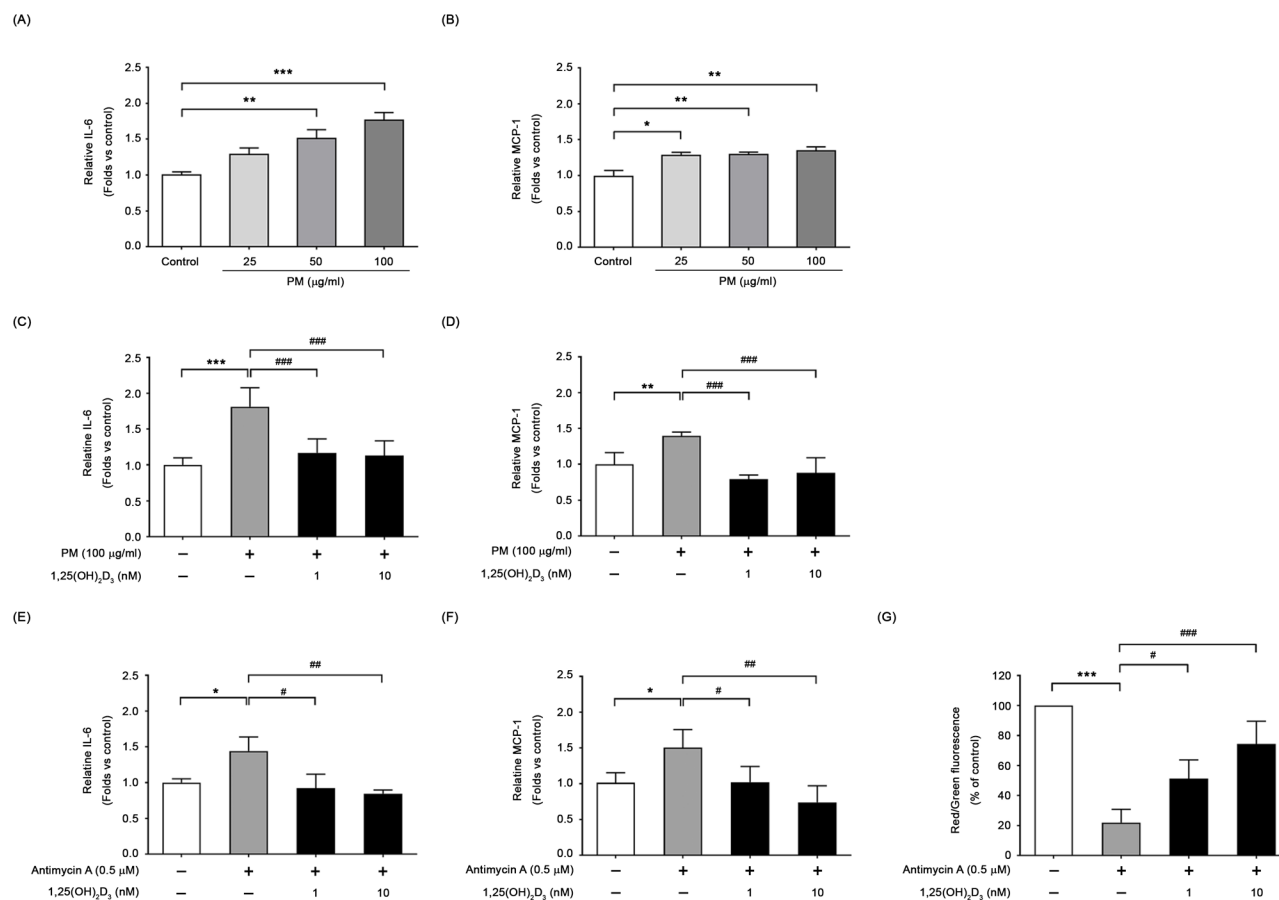
Fig. 7 $1,25(OH)_2D_3$ reduced the formation of inflammatory cytokines in PM stimulated BEAS-2B cultures. Culture supernatants were collected 24 h after PM stimulation without or with $1,25(OH)_2D_3$ pretreatment, and the concentrations of IL-6 and MCP-1 were measured. Concentration-dependent increases in IL-6 (**A**) and MCP-1 (**B**) were observed; however, addition of $1,25(OH)_2D_3$ reduced the release of inflammatory cytokines IL-6 (**C**) and MCP-1 (**D**). (**E**-**G**) In addition, $1,25(OH)_2D_3$ alleviated the generation of certain inflammatory cytokines triggered by antimycin A, which disrupts mitochondria with reduced membrane potential. Data were mean ± SD of three independent experiments. $^{***}P < 0.001$, $^{**}P < 0.01$ and $^*P < 0.05$ as compared with untreated cells (control)

disrupts mitochondrial function (Fig. 7E to G). These results demonstrate a protective role of $1,25(OH)_2D_3$ against PM-induced mitochondrial malfunction, and the consequent release of certain inflammatory cytokines, such as IL-6 and MCP-1.

Discussion

Our main findings demonstrate that $1,25(OH)_2D_3$ improves PM-induced perturbations in mitochondrial morphology and function, alterations in mtDNA-CN and consequent release of certain inflammatory cytokines, such as IL-6 and MCP-1, in human bronchial epithelial cells. Additionally, $1,25(OH)_2D_3$ restores intracellular calcium homeostasis, particularly within mitochondria, which are influenced by exposure to PM. The underlying mechanism of $1,25(OH)_2D_3$ involves in the upregulation of enzymatic (SOD1, SOD2 and CAT) and non-enzymatic (GSH and NADPH) antioxidants responding to counteract mitochondrial oxidative attack (Fig. 8).

In the present study, we provided evidence supporting the capacity of $1,25(OH)_2D_3$ in modulating the deleterious impacts of PM on bronchial epithelium. Our findings were in line with the Bose et al. epidemiological study shown that $1,25(OH)_2D_3$ insufficient obese children living in high PM environments have significantly increased odds of asthma [5]. In another epidemiological study of children with asthma, Rosser et al. have also reported $1,25(OH)_2D_3$ insufficiency is a risk factor for asthma exacerbations in children residing close to major roads [31]. An in vivo animal study has demonstrated that vitamin D supplementation had protective effect against the development of severe asthma when exposed to traffic-related particulate matter [4]. In a study using primary human bronchial epithelial cells (HBECs), Pfeffer et al. have shown the modulating property of $1,25(OH)_2D_3$ on oxidative stress and inflammatory responses by PM-stimulated HBECs [28]. While comparing data with previous researches, we provided new insights into the beneficial role of vitamin D in bronchial epithelial response to PM
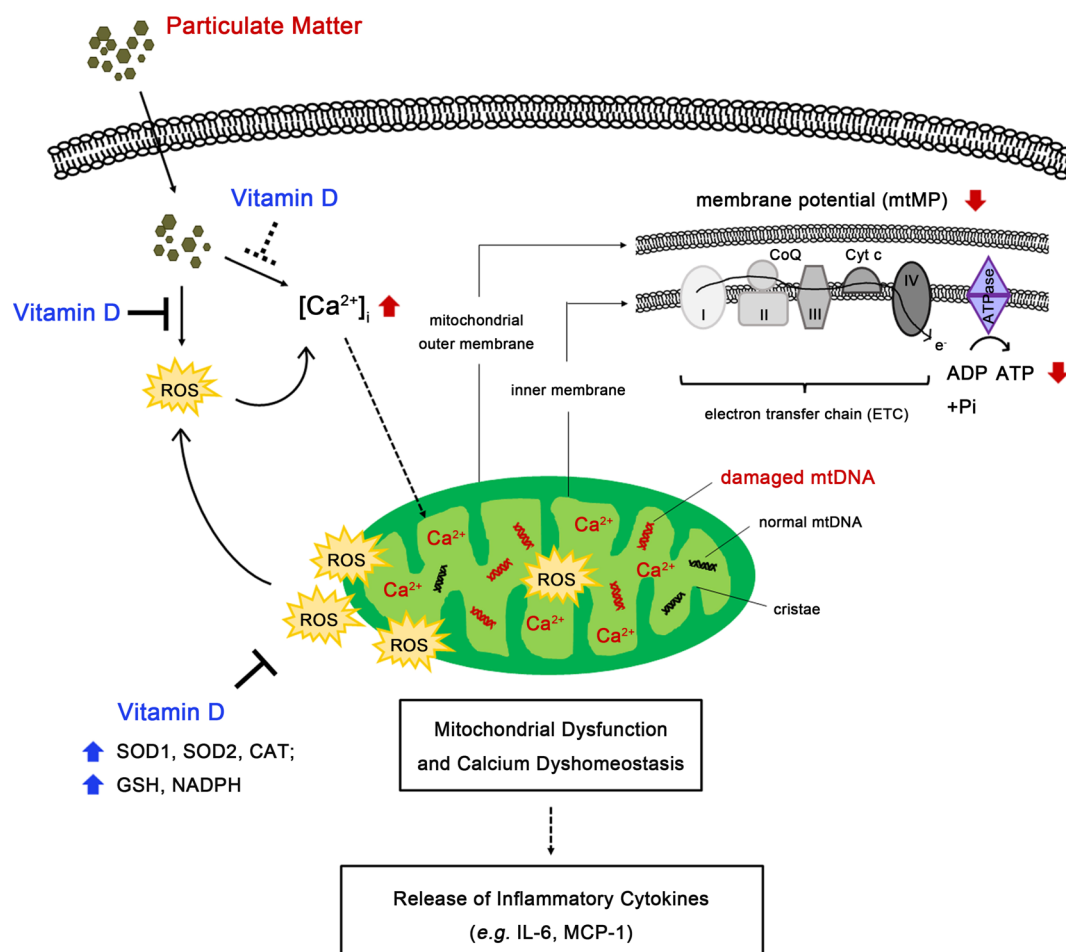
Fig. 8 A schematic illustration of the advantageous function of 1,25(OH)$_2$D$_3$ in enhancing epithelial defense against PM-induced mitochondrial ROS damages. Supplementation with 1,25(OH)$_2$D$_3$ ameliorates PM-induced mitochondrial malfunctions, calcium dyshomeostasis and inflammation by regulating mitochondrial ROS homeostasis through enhancing antioxidant responses in BEAS-2B cells. PM-induced detrimental impacts on mitochondria were shown in red-color texts or arrows. The beneficial regulation of 1,25(OH)$_2$D$_3$ were shown in blue-color texts or arrows

exposure by showing that 1,25(OH)$_2$D$_3$, enhances antioxidant responses and mitigates against mitochondrial oxidative stress, most likely contributing to alleviating mtDNA damage, mitochondrial malfunctioning and calcium dysregulation in PM-stimulated BEAS-2B cells.

The regulation of mtDNA-CN is crucial for preserving mitochondrial function [1]. Over the past decades, mtDNA-CN alteration on human pulmonary diseases, such as asthma and COPD, has been reported [7, 9]. Emerging evidence supports an association of exposure to PM with mtDNA-CN [3, 16, 17, 39]. Upon mitochondrial damages induced by PM, BEAS-2B cells may increase the mtDNA copy numbers compared to the controls, serving as a compensatory mechanism to partially address mitochondrial malfunctions [12, 24]. To our best knowledge, the effect of 1,25(OH)$_2$D$_3$ on PM-induced alteration in mtDNA-CN, has been under-investigated. In this study, we demonstrated that pretreatment with 1,25(OH)$_2$D$_3$ restored mtDNA-CN and mitochondrial ROS production to basal values. Similar to the suppressive effect of

1,25(OH)$_2$D$_3$, we found that MitoTEMPO suppressed the increased amount of mtDNA-CN in PM-stimulated cultures. Our findings suggest that 1,25(OH)$_2$D$_3$ plays a key role in protecting mtDNA from ROS attack and in preserving mtDNA-CN and mitochondrial functions due to its antioxidant capacity.

Previous studies have shown that multiple mitochondrial perturbations were induced by PM stimulation [34, 40, 46], but limited evidence is available regarding the role of 1,25(OH)$_2$D$_3$ playing in these deleterious effects of PM. In this study, we found that reducing mitochondrial ROS generation by adding MitoTEMPO, a mitochondrial ROS inhibitor, or 1,25(OH)$_2$D$_3$ to PM-exposed cells was closely connected to the subsequent reduction in intracellular ROS levels. This highlights that mitochondria are the primary contributors of ROS in PM-exposed cells [25]. Additionally, we observed that pretreatment with 1,25(OH)$_2$D$_3$ for 6 h upregulated the expression of oxidative stress-related genes, particularly SOD2 localized within the mitochondrial matrix [18], whereas exposure

to PM alone did not induce any changes. Furthermore, pretreatment with $1,25(OH)_2D_3$ partially restored the PM-induced increase in the protein expression of VDAC-1, a component of the mTPT [11]. Previous investigations suggest that mitochondria-generated ROS can induce the mTPT opening, initiating a regenerative cycle where mitochondrial ROS are continuously produced and released into the cytosol and neighboring mitochondria [45]. This feedback mechanism, known as ROS-induced ROS release (RIRR), can activate cellular signaling responses and induce mitochondrial damage [44, 45]. These findings highlight the significant role of mitochondrial-formed ROS in PM-induced mitochondrial perturbations. Our data suggest that $1,25(OH)_2D_3$ promotes the antioxidant response, directly targets mitochondria to downregulate VDAC-1 expression and mitigate a positive-feedback loop of mitochondrial ROS, consequently, alleviates mitochondrial ROS-triggered mitochondrial damage and subsequent inflammation in PM-exposed BEAS-2B cells. Several studies have reported that supplementation with antioxidants was protective against PM-induced mitochondrial injury [27, 33]. Our findings provide supportive evidence that $1,25(OH)_2D_3$ plays a protective role on mitochondrial metabolism in the context to PM exposure.

In addition to the principal role of $1,25(OH)_2D_3$ in maintaining calcium homeostasis [37], we evidenced that $1,25(OH)_2D_3$ mitigated the calcium-ROS self-amplifying loop to restore mitochondrial oxidative damages in PM-stimulated BEAS-2B cells. Our study demonstrated that the relationship between intracellular calcium accumulation and ROS overproduction in PM-stimulated cells leads to oxidative burst and mitochondrial injury. Moreover, perturbed mitochondria may lose the ability to buffer transient elevations in intracellular calcium induced by PM, resulting in the accumulation of mitochondrial calcium. The crosstalk between calcium and mitochondrial ROS had been shown previously [2, 14, 41]. We also observed that $1,25(OH)_2D_3$ restored certain degree of the increase of VDAC-1 protein expression induced by PM, suggesting a potential interplay between VDAC-1 and mitochondrial calcium homeostasis.

Conclusions
Our study highlights the advantageous function of $1,25(OH)_2D_3$ in controlling mitochondrial ROS homeostasis following exposure to PM. Supplementation of $1,25(OH)_2D_3$ protected BEAS-2B cells from mitochondrial malfunctioning, thereby preventing the release of certain inflammatory cytokines, such as IL-6 and MCP-1, and from calcium dyshomeostasis, particularly within mitochondria, through the enhancement of BEAS-2B antioxidant responses. Vitamin D sufficiency may be beneficial to optimize mitochondrial function, improve

the body's defense against air pollution, and reduce the development of air pollution-related respiratory diseases.

Abbreviations

$1,25(OH)_2D_3$	1, 25-dihydroxyvitamin D3
ATP	Adenosine triphosphate
AUC	Area under curve
B2M	β2-microglobulin
CAT	Catalase
COPD	Chronic obstructive pulmonary disease
Ct	Cycle threshold
DCF-DA	2′,7′-dichlorodihydrofluorescein diacetate
DMEM/F-12	Dulbecco's Modified Eagle's Medium/ Nutrient Mixture F-12
DMSO	Dimethyl sulfoxide
EDTA	Ethylenediaminetetraacetic acid
Ex/Em	Excitation/emission
FBS	Fetal bovine serum
Fluo-4 AM	Fluo-4 acetoxymethyl ester
GAPDH	Glyceraldehyde-3-phosphate dehydrogenase
GPX	Glutathione peroxidase
HBSS	Hanks' Balanced Salt Solution
MCP-1	Monocyte chemoattractant protein 1
MFI	Mean fluorescence intensity
mtDNA-CN	Mitochondrial DNA copy number
mtMP	Mitochondrial membrane potential
mTPT	Mitochondrial permeability transition pore
NAC	N-acetyl-L-cysteine
PAH	Polycyclic aromatic hydrocarbon
PBS	Phosphate-buffered saline
PM	Particulate matter
Rhod-2 AM	Rhodamine-2-acetoxymethyl ester
RIRR	ROS-induced ROS release
ROS	Reactive oxygen species
RT-qPCR	Reverse transcription-quantitative polymerase chain reaction
SOD	Superoxide dismutase
TEM	Transmission electron microscopy
tRNA	Transfer RNA
VDAC-1	Voltage-dependent anion channel 1
WST-1	Water-soluble tetrazolium 1

Author contributions
Ju Chang-Chien designed the experiments, performed the experiments, analyzed the results, and wrote the original manuscript. Jing-Long Huang and Hui-Ju Tsai provided resources and edited the manuscript. Shih-Ling Wang performed the experiments and co-analyzed the results. Ming-Ling Kuo co-supervised the study, interpreted the results, and edited the manuscript. Tsung-Chieh Yao conceived and supervised the study, interpreted the results, edited the manuscript, and acquired funding. All authors read and approved the final manuscript.

Chang-Chien *et al. Respiratory Research*   (2024) 25:321

Page 13 of 14

Data availability
The datasets used and/or analyzed during the current research are available from the corresponding upon reasonable request.

Declarations

Ethics approval and consent to participate
Not applicable

Consent for publication
Not applicable

Competing interests
The authors declare no competing interests

Author details
[1]Division of Allergy, Asthma, and Rheumatology, Department of Pediatrics, Chang Gung Memorial Hospital, 5 Fu-Hsin Street, Kweishan, Taoyuan 33305, Taiwan
[2]School of Medicine, Chang Gung University College of Medicine, Taoyuan, Taiwan
[3]Department of Pediatrics, New Taipei Municipal TuCheng Hospital, New Taipei, Taiwan
[4]Community Medicine Research Center, Chang Gung Memorial Hospital at Keelung, Keelung, Taiwan
[5]Institute of Population Health Sciences, National Health Research Institutes, Zhunan, Taiwan
[6]College of Life Science, National Tsing-Hua University, Hsinchu, Taiwan
[7]Department of Microbiology and Immunology, Graduate Institute of Biomedical Sciences, College of Medicine, Chang Gung University, 259 Wenhua 1st Road, Kweishan, Taoyuan 33302, Taiwan

References
1. Annesley SJ, Fisher PR. Mitochondria in health and disease. Cells. 2019;8. https://doi.org/10.3390/cells8070680.
2. Aon MA, Cortassa S, Marban E, et al. Synchronized whole cell oscillations in mitochondrial metabolism triggered by a local release of reactive oxygen species in cardiac myocytes. J Biol Chem. 2003;278:44735–44. https://doi.org/10.1074/jbc.M302673200.
3. Aviles-Ramirez C, Moreno-Godinez ME, Bonner MR, et al. Effects of exposure to environmental pollutants on mitochondrial DNA copy number: a meta-analysis. Environ Sci Pollut Res Int. 2022;29:43588–606. https://doi.org/10.1007/s11356-022-19967-5.
4. Bolcas PE, Brandt EB, Zhang Z, et al. Vitamin D supplementation attenuates asthma development following traffic-related particulate matter exposure. J Allergy Clin Immunol. 2019;143:386–e394383. https://doi.org/10.1016/j.jaci.2018.04.042.
5. Bose S, Diette GB, Woo H, et al. Vitamin D status modifies the response to indoor particulate matter in obese urban children with asthma. J Allergy Clin Immunol Pract. 2019;7:1815–e18221812. https://doi.org/10.1016/j.jaip.2019.01.051.
6. Brisac C, Teoule F, Autret A, et al. Calcium flux between the endoplasmic reticulum and mitochondrion contributes to poliovirus-induced apoptosis. J Virol. 2010;84:12226–35. https://doi.org/10.1128/JVI.00994-10.
7. Carpagnano GE, Lacedonia D, Malerba M, et al. Analysis of mitochondrial DNA alteration in new phenotype ACOS. BMC Pulm Med. 2016;16:31. https://doi.org/10.1186/s12890-016-0192-6.
8. Chambers ES, Hawrylowicz CM. The impact of vitamin D on regulatory T cells. Curr Allergy Asthma Rep. 2011;11:29–36. https://doi.org/10.1007/s11882-010-0161-8.
9. Cocco MP, White E, Xiao S, et al. Asthma and its relationship to mitochondrial copy number: results from the Asthma Translational Genomics Collaborative (ATGC) of the Trans-Omics for Precision Medicine (TOPMed) program. PLoS ONE. 2020;15:e0242364. https://doi.org/10.1371/journal.pone.0242364.
10. El Taieb MA, Fayed HM, Aly SS, et al. Assessment of serum 25-hydroxyvitamin d levels in children with atopic dermatitis: correlation with SCORAD index. Dermatitis. 2013;24:296–301. https://doi.org/10.1097/DER.0000000000000010.
11. Endlicher R, Drahota Z, Stefkova K, et al. The mitochondrial permeability transition pore-current knowledge of its structure, function, and regulation, and optimized methods for evaluating its functional state. Cells. 2023;12. https://doi.org/10.3390/cells12091273.
12. Fu Y, Tigano M, Sfeir A. Safeguarding mitochondrial genomes in higher eukaryotes. Nat Struct Mol Biol. 2020;27:687–95. https://doi.org/10.1038/s41594-020-0474-9.
13. Gaudet M, Plesa M, Mogas A, et al. Recent advances in vitamin D implications in chronic respiratory diseases. Respir Res. 2022;23:252. https://doi.org/10.1186/s12931-022-02147-x.
14. Gorlach A, Bertram K, Hudecova S, et al. Calcium and ROS: a mutual interplay. Redox Biol. 2015;6:260–71. https://doi.org/10.1016/j.redox.2015.08.010.
15. Heinrich J, Schikowski T. COPD patients as vulnerable subpopulation for exposure to ambient air pollution. Curr Environ Health Rep. 2018;5:70–6. https://doi.org/10.1007/s40572-018-0178-z.
16. Hou L, Zhang X, Dioni L, et al. Inhalable particulate matter and mitochondrial DNA copy number in highly exposed individuals in Beijing, China: a repeated-measure study. Part Fibre Toxicol. 2013;10:17. https://doi.org/10.1186/1743-8977-10-17.
17. Hu C, Sheng X, Li Y, et al. Effects of prenatal exposure to particulate air pollution on newborn mitochondrial DNA copy number. Chemosphere. 2020;253:126592. https://doi.org/10.1016/j.chemosphere.2020.126592.
18. Ighodaro OM, Akinloye OA. First line defence antioxidants-superoxide dismutase (SOD), catalase (CAT) and glutathione peroxidase (GPX): their fundamental role in the entire antioxidant defence grid. Alexandria J Med. 2019;54:287–93. https://doi.org/10.1016/j.ajme.2017.09.001.
19. Jin X, Xue B, Zhou Q, et al. Mitochondrial damage mediated by ROS incurs bronchial epithelial cell apoptosis upon ambient PM2.5 exposure. J Toxicol Sci. 2018;43:101–11. https://doi.org/10.2131/jts.43.101.
20. Jones DP. Radical-free biology of oxidative stress. Am J Physiol Cell Physiol. 2008;295:C849–868. https://doi.org/10.1152/ajpcell.00283.2008.
21. Kobayashi S, Yoda Y, Takagi H, et al. Short-term effects of the chemical components of fine particulate matter on pulmonary function: a repeated panel study among adolescents. Sci Total Environ. 2023;895:165195. https://doi.org/10.1016/j.scitotenv.2023.165195.
22. Kuo CY, Chan CK, Wu CY, et al. The short-term effects of ambient air pollutants on childhood asthma hospitalization in Taiwan: a national study. Int J Environ Res Public Health. 2019;16. https://doi.org/10.3390/ijerph16020203.
23. Lai TC, Chen YC, Cheng HH, et al. Combined exposure to fine particulate matter and high glucose aggravates endothelial damage by increasing inflammation and mitophagy: the involvement of vitamin D. Part Fibre Toxicol. 2022;19(25). https://doi.org/10.1186/s12989-022-00462-1.
24. Li Y, Sundquist K, Wang X, et al. Association of mitochondrial DNA copy number and telomere length with prevalent and incident cancer and cancer mortality in women: a prospective Swedish population-based study. Cancers (Basel). 2021;13. https://doi.org/10.3390/cancers13153842.
25. Murphy MP. How mitochondria produce reactive oxygen species. Biochem J. 2009;417:1–13. https://doi.org/10.1042/BJ20081386.
26. Murphy MP, Holmgren A, Larsson NG, et al. Unraveling the biological roles of reactive oxygen species. Cell Metab. 2011;13:361–6. https://doi.org/10.1016/j.cmet.2011.03.010.
27. Pardo M, Xu F, Shemesh M, et al. Nrf2 protects against diverse PM(2.5) components-induced mitochondrial oxidative damage in lung cells. Sci Total Environ. 2019;669:303–13. https://doi.org/10.1016/j.scitotenv.2019.01.436.
28. Pfeffer PE, Lu H, Mann EH, et al. Effects of vitamin D on inflammatory and oxidative stress responses of human bronchial epithelial cells exposed to particulate matter. PLoS ONE. 2018;13:e0200040. https://doi.org/10.1371/journal.pone.0200040.
29. Piao MJ, Ahn MJ, Kang KA, et al. Particulate matter 2.5 damages skin cells by inducing oxidative stress, subcellular organelle dysfunction, and apoptosis. Arch Toxicol. 2018;92:2077–91. https://doi.org/10.1007/s00204-018-2197-9.

30 Rooney JP, Ryde IT, Sanders LH, et al. PCR based determination of mitochondrial DNA copy number in multiple species. Methods Mol Biol. 2015;1241:23–38. https://doi.org/10.1007/978-1-4939-1875-1_3.

31 Rosser F, Brehm JM, Forno E, et al. Proximity to a major road, vitamin D insufficiency, and severe asthma exacerbations in Puerto Rican children. Am J Respir Crit Care Med. 2014;190:1190–3. https://doi.org/10.1164/rccm.201408-1568LE.

32 Rossi A, Pizzo P, Filadi R. Calcium, mitochondria and cell metabolism: a functional triangle in bioenergetics. Biochim Biophys Acta Mol Cell Res. 2019;1866:1068–78. https://doi.org/10.1016/j.bbamcr.2018.10.016.

33 Soberanes S, Misharin AV, Jairaman A, et al. Metformin targets mitochondrial electron transport to reduce air-pollution-induced thrombosis. Cell Metab. 2019;29:335–e347335. https://doi.org/10.1016/j.cmet.2018.09.019.

34 Sotty J, Kluza J, De Sousa C, et al. Mitochondrial alterations triggered by repeated exposure to fine (PM(2.5 – 0.18)) and quasi-ultrafine (PM(0.18)) fractions of ambient particulate matter. Environ Int. 2020;142:105830. https://doi.org/10.1016/j.envint.2020.105830.

35 Szabo I, Szewczyk A. Mitochondrial ion channels. Annu Rev Biophys. 2023;52:229–54. https://doi.org/10.1146/annurev-biophys-092622-094853.

36 Tilokani L, Nagashima S, Paupe V, et al. Mitochondrial dynamics: overview of molecular mechanisms. Essays Biochem. 2018;62:341–60. https://doi.org/10.1042/EBC20170104.

37 Veldurthy V, Wei R, Oz L, et al. Vitamin D, calcium homeostasis and aging. Bone Res. 2016;4:16041. https://doi.org/10.1038/boneres.2016.41.

38 Veskoukis AS, Margaritelis NV, Kyparos A, et al. Spectrophotometric assays for measuring redox biomarkers in blood and tissues: the NADPH network. Redox Rep. 2018;23:47–56. https://doi.org/10.1080/13510002.2017.1392695.

39 Wang X, Hart JE, Liu Q, et al. Association of particulate matter air pollution with leukocyte mitochondrial DNA copy number. Environ Int. 2020a;141:105761. https://doi.org/10.1016/j.envint.2020.105761.

40 Wang Y, Wu T, Tang M. Ambient particulate matter triggers dysfunction of subcellular structures and endothelial cell apoptosis through disruption of redox equilibrium and calcium homeostasis. J Hazard Mater. 2020b;394:122439. https://doi.org/10.1016/j.jhazmat.2020.122439.

41 Yan Y, Wei CL, Zhang WR, et al. Cross-talk between calcium and reactive oxygen species signaling. Acta Pharmacol Sin. 2006;27:821–6. https://doi.org/10.1111/j.1745-7254.2006.00390.x.

42 Yao TC, Tu YL, Chang SW, et al. Serum 25-hydroxyvitamin D levels in relation to lung function and exhaled nitric oxide in children. J Pediatr. 2014;165:1098–e11031091. https://doi.org/10.1016/j.jpeds.2014.08.048.

43 Yao TC, Huang HY, Pan WC, et al. Association of prenatal exposure to fine particulate matter pollution with childhood eczema. Allergy. 2021;76:2241–5. https://doi.org/10.1111/all.14738.

44 Zorov DB, Filburn CR, Klotz LO, et al. Reactive oxygen species (ROS)-induced ROS release: a new phenomenon accompanying induction of the mitochondrial permeability transition in cardiac myocytes. J Exp Med. 2000;192:1001–14. https://doi.org/10.1084/jem.192.7.1001.

45 Zorov DB, Juhaszova M, Sollott SJ. Mitochondrial reactive oxygen species (ROS) and ROS-induced ROS release. Physiol Rev. 2014;94:909–50. https://doi.org/10.1152/physrev.00026.2013.

46 Zou L, Li B, Xiong L, et al. Urban fine particulate matter causes cardiac hypertrophy through calcium-mediated mitochondrial bioenergetics dysfunction in mice hearts and human cardiomyocytes. Environ Pollut. 2022;305:119236. https://doi.org/10.1016/j.envpol.2022.119236.

Publisher's Note